Hindawi
International Journal of Aerospace Engineering
Volume 2019, Article ID 9563596, 15 pages
https://doi.org/10.1155/2019/9563596

Research Article

Assembly Variation Analysis of Aircraft Panels under Part-to-part Locating Scheme

Xia Liu[1], **Luling An**[1], **Zhiguo Wang**[1], **Changbai Tan**[2], **Xiaoping Wang**[1] **and Shouxin Yu**[1]

[1]*Nanjing University of Aeronautics and Astronautics, Jiangsu Key Laboratory of Precision and Micro-Manufacturing Technology, Nanjing 210016, China*
[2]*College of Engineering, University of Michigan, Ann Arbor 48105, USA*

Correspondence should be addressed to Luling An; anllme@nuaa.edu.cn

Received 15 September 2018; Revised 14 November 2018; Accepted 28 November 2018; Published 31 March 2019

Academic Editor: Jose Carlos Páscoa

A typical aircraft panel is the assembly consisting of a multitude of thin and lightweight compliant parts. In panel assembly process, part-to-part locating scheme has been widely adopted in order to reduce fixtures. By this locating scheme, a part is located onto the pre-fixed part/subassembly by determinant assembly (DA) holes, and temporary fasteners (e.g., spring pin) are used for joining these DA hole-hole pairs. The temporary fasteners can fasten DA hole-hole pairs in the axial and radial directions of DA holes. The fastening in the radial directions is realized by the expansion of temporary fasteners. Although the usage of temporary fasteners helps reduce the positional differences between hole-hole pairs, their clamping forces thereby may lead to elastic deformation of compliant parts/subassemblies. Limited research has been conducted on such elastic deformation produced by temporary fastener and its influence on assembly dimensional quality. This paper proposes a novel rigid-compliant variation analysis method for aircraft panel assembly, incorporating the deformation in part-to-part locating process. Based on the kinematic theory and linear elasticity deformation assumption, the variation propagation through the locating process, as well as the entire assembly process of an aircraft panel, is formulated. Then, the statistical variation analysis is performed with Monte Carlo (MC) simulation. Finally, the proposed method is validated by a case study. The result shows the deformation in the part-to-part locating process significantly impacts the assembly variations, and our method can provide a more accurate and reliable prediction.

1. Introduction

As a class of major structures in aircraft manufacturing, aircraft panels are widely used to build fuselages, wings, cabin doors and other large parts. Structurally, an aircraft panel is assembled with a multitude of compliant parts, which is characterized to be large, thin and lightweight. The dimensional accuracy of aircraft panel assembly is directly related to key characteristics (e.g., aerodynamics and fatigue durability) and safety of the aircraft. Assembly variation analysis is aimed at predicting the geometrical variations of an assembly system at early product design stage, which provide the mathematical basis to control and improve geometrical quality [1].

In the last two decades, rigid and compliant assembly variation analyses have been developed in parallel [2]. Rigid assembly variation is usually modeled based on the kinematics theory, where parts are assumed to be rigid. Jin and Shi [3] developed the dimensional variation analysis of sheet metal assembly by using state space model, while Mantripragada and Whitney [4] used state transition model to study the variation propagation in mechanical assemblies. Ding et al. [5] and Li et al. [6] conducted the sensitivity-based variation analysis for multi-station assembly process. Huang et al. [7, 8] developed three-dimensional (3D) stream-of-variation analysis (SOVA) for single-station and multi-station assemblies. Liu et al. [9] adopted differential motion vector to represent variations and formulate variation propagation. Qu et al. [10] introduced locating datum variations into multi-station assembly analysis. In such methods, part deformation is not taken into account in assembly variation analysis.

As to compliant variation analysis, parts are assumed to be deformable, and assembly variation propagation is modeled by mechanic principles. Liu and Hu [11] developed the method of influence coefficients (MIC) to establish the linear relationship between the variations of individual parts and assembly, under the assumption of linear elastic deformation. Camelio et al. [12] and Yue et al. [13] used a state space representation to extend the MIC in multi-station assembly system. Dahlstrom and Lindkvist [14], Xie et al. [15], and Lindau et al. [16] incorporated the contact effect of parts into assembly variation modeling. Yu et al. [17] discussed the effect of material variations (i.e., thickness of sheet) in sheet metal assembly, while Chen et al. [18] formulated the coupling effect of geometrical and material variations in compliant assembly. Wärmefjord et al. [19, 20] modeled different joining processes in assembly variation simulation of nonrigid parts and predicted required assembly forces and holding forces during the joining processes. Söderberg et al. [21] investigated the influence of variations of spot weld positions on the geometrical variation of an assembled product. Moos and Vezzetti [22] integrated the effect of material plasticity into finite element (FE) simulation of welding process. Lorin et al. [23] and Söderberg et al. [24] introduced MIC into stress calculation during assembly of composite parts.

Few studies can be found about mixed rigid-compliant assembly variation modeling. Ni et al. [25] developed a 3D precision analysis of sheet metal assembly, where rigid and compliant variations were computed by kinematic formulations and modified finite element analysis (FEA), respectively. Cai and Qiao [26] modeled the rigid-compliant hybrid variation propagation in sheet metal assembly, based on homogeneous transformation matrix (HTM) and MIC.

In recent years, increasing research efforts have been put on the variation analysis of aircraft panel assembly. Cheng et al. [27] analyzed the assembly variation propagation of aeronautical thin-walled structures under automated riveting process. Lin et al. [28] employed the substructure to reduce the complexity of FE modeling, while achieving a comparable prediction accuracy of assembly variations as complete FEA. Zheng et al. [29] established an equivalent mechanic model of riveting process to improve the computational efficiency of assembly variation analysis.

Traditionally, aircraft panel assembly requires numerous fixtures to locate the constituent parts. In order to reduce assembly fixtures, and to save time and cost, a technical trend in aircraft assembly is to adopt part-to-part locating scheme. Under part-to-part locating scheme, a part is directly located onto another part/subassembly by assembly features (AFs). Most commonly used AFs are round holes pair wisely made on separate parts, and these locating holes are called determinant assembly (DA) holes in aeronautical industry [30, 31]. Temporary fasteners (e.g., spring pin) are adopted to join the DA hole-hole pairs until riveting process is completed. The temporary fasteners can fasten the DA hole-hole pairs in the axial and radial directions of the DA holes. The fastening in the radial directions is realized by the expansion of the temporary fasteners, which results in the clamping forces on parts along the radial directions of the DA holes. Since the dimensional variations of predrilled DA holes and the positional differences between DA hole-hole pairs are technically inevitable, the clamping forces exerted by temporary fasteners may produce the deformation of compliant parts in this locating process. Unfortunately, such deformation is deliberately ignored to simplify the assembly variation model [32], or not sufficiently elaborated [28] in the existing studies. To the best of our knowledge, the deformation produced by temporary fasteners and its influence on assembly dimensional quality have not been investigated systematically and incorporated into the assembly variation analysis of compliant parts in existing research. To fulfill the strict dimensional accuracy requirement in aircraft manufacturing, a reliable assembly variation prediction by considering the deformation in part-to-part locating process becomes especially important for effective dimensional management of aircraft assembly.

Assembly variations due to both rigid motions and compliant deformation exist in aircraft panels. This paper proposes a method for rigid-compliant assembly variation analysis of aircraft panel under part-to-part locating scheme. This method is developed by using a typical aircraft panel assembly, where the frame parts, such as stringer, clip and sheet frame, are located by DA holes. Firstly, the variation propagation in part-to-part locating process is modeled based on the kinematic theory and MIC, where the deformation produced by the clamping forces of temporary fasteners is incorporated. Then, the variation propagation through the entire assembly process of a panel is modeled, and the statistical variation analysis is performed by using Monte Carlo (MC) simulation.

The paper is organized as follows. Section 2 will give the problem definition and mathematical representation. Section 3 will analyze the variation propagation in part-to-part locating process. Section 4 will model the variation propagation through the entire assembly process of an aircraft panel and conduct the statistical variation analysis. Section 5 will validate the proposed method with a case study. Section 6 will conclude our study.

2. Problem Definition and Mathematical Representation

2.1. Problem Description and Assumption. As shown in Figure 1, a typical aircraft panel is composed of a number of sheet metals, including skins, stringers, clips and sheet frames. Its entire assembly process includes two stations. In Station 1, skins, stringers and clips are assembled into a subassembly. In Station 2, sheet frames are assembled with the subassembly into a panel assembly. Here, the skins and the subassembly in Stations 1 and 2 are located by fixture, while the frame parts are all located by the DA holes. Each of the stringers and clips is located onto the skins by two DA holes, while each sheet frame is located onto the clips by three DA holes.

In the aircraft panel assembly with part-to-part locating, two or more pairs of DA holes are used to locate a part onto

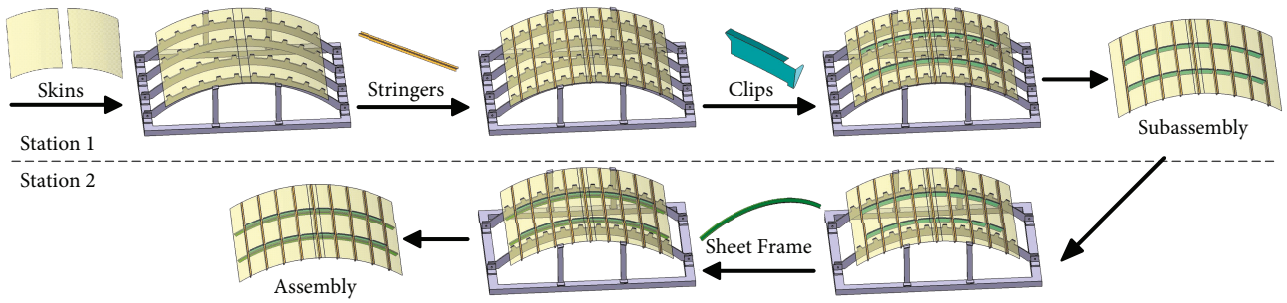

Figure 1: Assembly process of an aircraft panel.

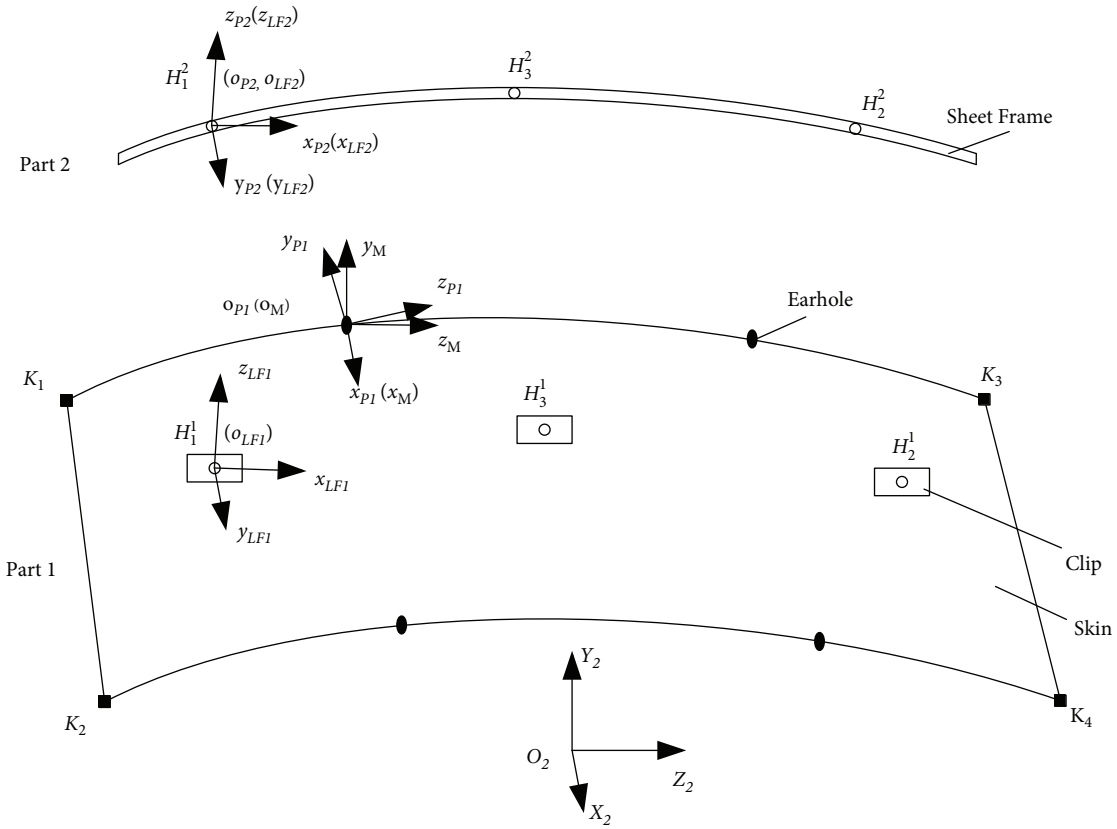

Figure 2: A subassembly and a sheet frame.

the pre-fixed part/subassembly. The DA hole-hole pairs are joined together by temporary fasteners. The temporary fasteners are inserted and then fasten the paired DA holes. The expansion of the fasteners results in the clamping forces along the radial directions of the DA holes. In the practical operation, these clamping forces are exerted highly dependent on the assembly operator's experience. In this situation, plastic deformation of parts/subassemblies is not allowed, but small elastic deformation cannot be avoided. The clamping forces of the temporary fasteners coupled with the inevitable positional differences between the DA hole-hole pairs may produce the elastic deformation of parts/subassemblies.

In this case, the elastic deformation of the sheet frames may have a higher possibility than that of the stringers and clips in the part-to-part locating process, this is because (a) the number of DA holes is more, and (b) the DA hole-hole pairs of the sheet frames may have larger positional differences, where the positional variations of the located DA holes on the clips are propagated and accumulated through multiple parts and multiple stations. Therefore, a sheet frame is taken as an example to illustrate the variation propagation in part-to-part locating process.

As shown in Figure 2, in Station 2, a subassembly from Station 1 is referred to as Part 1, and a sheet frame is referred to as Part 2. For simplicity, only the clips with the located DA holes, as well as the skins, are shown for Part 1. Part 1 is located onto the fixture by earholes and fixture boards, and Part 2 will be located onto Part 1 by three DA holes.

The centers of the DA holes of Part 1 are denoted as H_1^1, H_2^1 and H_3^1. Similarly, the centers of Part 2 are denoted as H_1^2, H_2^2 and H_3^2. The measuring points, denoted as K_1~K_4, are defined on the skins. Their variations are used to represent the assembly variations.

Part deformation is also influenced by the locating sequence of DA holes. Here, H_1^2, H_2^2 and H_3^2 on Part 2 are defined as the principal, secondary and tertiary datum holes, respectively. It is assumed that the principal datum hole is firstly located, and then the other DA holes are located in sequence.

Notably, to highlight our research focus, some assumptions are made as follows:

(1) The part deformation in assembly is small and linearly elastic without plastic deformation or buckling

(2) The influences of friction, contact force, gravity, etc. are neglected

(3) The local deformation around riveting holes and DA holes is neglected

(4) The dimension and shape of DA holes stay unchanged

2.2. Mathematical Representation

2.2.1. Definition of Coordinate Systems. In order to describe the variations as well as their relationships, four types of coordinate systems (CSs) are defined, including station coordinate system (SCS), part coordinate system (PCS), location feature coordinate system (LFCS) and measurement coordinate system (MCS).

SCS is considered to be error free and unchangeable during the assembly process of a station. PCS is associated with a part, while LFCS is associated with DA holes for part-to-part locating, which contains the ones of locating and located DA holes. For a part to be located with the DA holes, the LFCS of locating DA holes is on this part, which is defined that: the origin is in the center of the principal datum hole; the x-axis points to the center of the secondary datum hole; if the tertiary datum hole exists and is noncollinear with the principal and secondary datum holes, the y-axis is perpendicular to the plane which is determined by the centers of the principal, secondary and tertiary datum holes. Similarly, the LFCS of located DA holes on the pre-fixed part/subassembly corresponds to the one of locating DA holes. MCS is defined as the coordinate system in which the assembly variations are measured. Moreover, the spatial relationships among different CSs can be described by HTM [26].

As shown in Figure 2, $O_2X_2Y_2Z_2$ is the SCS_2 of Station 2, where the fixture is assumed to be fixed. $o_{P1}x_{P1}y_{P1}z_{P1}$ and $o_{P2}x_{P2}y_{P2}z_{P2}$ are the PCSs of Parts 1 and 2, denoted as PCS_1 and PCS_2, respectively. On Parts 1 and 2, $o_{LF1}x_{LF1}y_{LF1}z_{LF1}$ and $o_{LF2}x_{LF2}y_{LF2}z_{LF2}$ are the LFCSs of located and locating DA holes, denoted as $LFCS_1$ and $LFCS_2$, respectively. $o_Mx_My_Mz_M$ on Part 1 is the MCS. Because the locating DA holes are not only the locating datum but also the measurement datum of Part 2, PCS_2 is assumed to be coincided with $LFCS_2$, PCS_1 and MCS are defined similarly with the LFCS, which take two and three of the earholes as reference points, respectively.

Due to the positional variations of DA holes and earholes, PCS, LFCS and MCS are all divided into nominal and actual ones, respectively. The former ones are decorated with a superscript "n." In particular, the principal datum holes of locating DA holes are assumed to be free of position variations. Furthermore, the HTMs of ${}^{n}PCS_1$, ${}^{n}PCS_2$ (${}^{n}LFCS_2$), ${}^{n}LFCS_1$ and ${}^{n}MCS$, with respect to (w.r.t.) SCS_2, are $\mathbf{T}_{nP1}^{S2}$, $\mathbf{T}_{nP2}^{S2}$, $\mathbf{T}_{nLF1}^{S2}$ and $\mathbf{T}_{nM}^{S2}$. Obviously, $\mathbf{T}_{nP2}^{S2} = \mathbf{T}_{nLF1}^{S2}$.

2.2.2. Variation Representation and Calculation. The dimensional and geometric variation indicates the deviation of an actual feature from its nominal one. The rotations and translations of a feature can be described by small displacement torsor (SDT) model [33, 34]. In SDT model, feature variations are defined as vectorial representation [35], i.e., $\boldsymbol{\tau} = [\boldsymbol{\omega} \quad \boldsymbol{\varepsilon}]^{\mathrm{T}}$. $\boldsymbol{\omega} = [\alpha \quad \beta \quad \gamma]^{\mathrm{T}}$ denotes the rotation vector, which has three components: α, β and γ around x-, y-, and z-axes, respectively. Similarly, $\boldsymbol{\varepsilon} = [u \quad v \quad w]^{\mathrm{T}}$ denotes the translation vector, which has three components: u, v and w along x-, y- and z-axes, respectively.

The assembly variations are introduced by variation sources which are propagated and accumulated through the assembly process. In a rigid variation analysis based on the kinematic theory [4, 9, 36], for example, the variation of feature i is $\boldsymbol{\tau}_i = [\boldsymbol{\omega}_i \quad \boldsymbol{\varepsilon}_i]^{\mathrm{T}}$. An arbitrary point on feature i is A, and its coordinates are denoted as $\mathbf{a} = [x_a \quad y_a \quad z_a]^{\mathrm{T}}$. The variation of point A can be calculated with HTM [37, 38] as follows:

$$[\Delta\mathbf{a} \quad 1]^{\mathrm{T}} = \mathbf{T}_i[\mathbf{a} \quad 1]^{\mathrm{T}} - [\mathbf{a} \quad 1]^{\mathrm{T}}, \tag{1}$$

where the HTM $\mathbf{T}_i$ is

$$\mathbf{T}_i = \begin{bmatrix} \mathbf{R}_i & \boldsymbol{\varepsilon}_i \\ \mathbf{0} & 1 \end{bmatrix}, \tag{2}$$

and $\mathbf{R}_i$ is

$$\boldsymbol{R}_i = \begin{bmatrix} \cos\beta_i\cos\gamma_i & -\cos\beta_i\sin\gamma_i & \sin\beta_i \\ \sin\alpha_i\sin\beta_i\cos\gamma_i + \cos\alpha_i\sin\gamma_i & -\sin\alpha_i\sin\beta_i\sin\gamma_i + \cos\alpha_i\cos\gamma_i & -\sin\alpha_i\cos\beta_i \\ -\cos\alpha_i\sin\beta_i\cos\gamma_i + \sin\alpha_i\sin\gamma_i & \cos\alpha_i\sin\beta_i\sin\gamma_i + \sin\alpha_i\cos\gamma_i & \cos\alpha_i\cos\beta_i \end{bmatrix}. \tag{3}$$

When α_i, β_i, and γ_i are very small, equation (3) is

$$\mathbf{R}_i \approx \begin{bmatrix} 1 & -\gamma_i & \beta_i \\ \gamma_i & 1 & -\alpha_i \\ -\beta_i & \alpha_i & 1 \end{bmatrix}. \tag{4}$$

In compliant variation analysis based on MIC [11, 12], the linear relationships between the displacements $\mathbf{V}$ and forces $\mathbf{F}$ of certain points can be formulated as follows:

$$\begin{bmatrix} \mathbf{F}_{cF}^{\mathrm{T}} & \mathbf{F}_{cV}^{\mathrm{T}} \end{bmatrix}^{\mathrm{T}} = \mathbf{K} \begin{bmatrix} \mathbf{V}_{cF}^{\mathrm{T}} & \mathbf{V}_{cV}^{\mathrm{T}} \end{bmatrix}^{\mathrm{T}}, \tag{5}$$

where the stiffness matrix $\mathbf{K}$ corresponds to the characteristics on the boundary condition during assembly process, and the formulated points are divided into two categories: (a) the displacements and forces decorated with a subscript "cF" correspond to the points which are subject to constant loads, and (b) the displacements and forces decorated with a subscript "cV" represent that the displacements of the points remain constant. Here, $\mathbf{K}$ for certain points can be directly extracted by commercial FE software, except the one for the points defined as the boundary condition. Certainly, the forces on the boundary condition points, denoted as $\mathbf{F}_B$, have the linear relationships to the forces on other points, as follows:

$$\mathbf{F}_B = \mathbf{C} \begin{bmatrix} \mathbf{F}_{cF}^{\mathrm{T}} & \mathbf{F}_{cV}^{\mathrm{T}} \end{bmatrix}^{\mathrm{T}}, \tag{6}$$

where $\mathbf{C}$ is the coefficient matrix, which can be obtained from commercial FE software.

From equations (5) and (6), $\mathbf{V}_{cF}$, $\mathbf{F}_{cV}$ and $\mathbf{F}_B$ can be calculated with the constants $\mathbf{F}_{cF}$ and $\mathbf{V}_{cV}$.

3. Variation Propagation Analysis in Part-to-Part Locating Process

In the part-to-part locating process, the compliant parts/-subassemblies may be deformed, due to the positional differences between DA hole-hole pairs and the clamping forces of temporary fasteners. The variation propagation analysis is aimed at studying the introduction, propagation and accumulation of data stream of variations through an assembly process. In this section, incorporating and not incorporating the deformation of parts/subassemblies, the methods of variation propagation analysis in part-to-part locating process are both proposed, based on the kinematic theory and MIC.

3.1. Variation Propagation Analysis Not Incorporating Deformation. Not incorporating the deformation in part-to-part locating process, the variation analysis is an overall rigid one. According to the locating sequence of DA holes, the rigid locating process is regarded as follows:

(1) The principal datum hole of Part 2 is fastened with its located DA hole on Part 1, to ensure that this DA hole-hole pair is coincident, i.e., H_1^2 is coincident with H_1^1

(2) The secondary datum hole of Part 2 is fastened with its located DA hole on Part 1, to make the distance between the centers of this DA hole-hole pair minimized. Here, H_2^2 is collinear with H_1^1 and H_2^1

(3) The tertiary datum hole of Part 2 is fastened with its located DA hole on Part 1, where H_3^2 is regarded to be in the plane determined by H_1^1, H_2^1 and H_3^1, to minimize the distance between the centers of this DA hole-hole pair

Therefore, the rigid locating process is assumed that: PCS_2 is translated and rotated to be coincident with LFCS_1, and then the degrees of freedom (DOFs) of the DA hole-hole pair centers are tied.

As shown in Figure 2, the coordinates of H_i^1, $i = 1,2,3$, w.r.t. SCS_2, are $\mathbf{H}_{1i}^{S2} = \begin{bmatrix} X_{h1i}^{S2} & Y_{h1i}^{S2} & Z_{h1i}^{S2} \end{bmatrix}^{\mathrm{T}}$. The coordinates of H_i^2, $i = 1,2,3$, w.r.t. ${}^{\mathrm{n}}\mathrm{PCS}_2$, are $\mathbf{H}_{2i}^{nP2} = \begin{bmatrix} x_{h2i}^{nP2} & y_{h2i}^{nP2} & z_{h2i}^{nP2} \end{bmatrix}^{\mathrm{T}}$, and they w.r.t. PCS_2 are $\mathbf{H}_{2i}^{P2} = \begin{bmatrix} x_{h2i}^{P2} & y_{h2i}^{P2} & z_{h2i}^{P2} \end{bmatrix}^{\mathrm{T}}$ as follows:

$$\begin{bmatrix} \left(\mathbf{H}_{2i}^{P2}\right)^{\mathrm{T}} & 1 \end{bmatrix}^{\mathrm{T}} = \mathbf{T}_{nP2}^{P2} \begin{bmatrix} \left(\mathbf{H}_{2i}^{nP2}\right)^{\mathrm{T}} & 1 \end{bmatrix}^{\mathrm{T}}, \quad i = 1, 2, 3, \tag{7}$$

where $\mathbf{H}_{21}^{P2} = \mathbf{0}$, $y_{h22}^{P2} = 0$, $z_{h22}^{P2} = 0$, $y_{h23}^{P2} = 0$, and $\mathbf{T}_{nP2}^{P2}$ are the HTM of ${}^{\mathrm{n}}\mathrm{PCS}_2$ w.r.t. PCS_2. Coupled with equation (4), $\mathbf{T}_{nP2}^{P2}$ and $\mathbf{H}_{2i}^{P2}$, $i = 1,2,3$, can be calculated.

Similarly, the HTM of ${}^{\mathrm{n}}\mathrm{LFCS}_1$ w.r.t. LFCS_1 denoted as $\mathbf{T}_{nLF1}^{LF1}$, as well as the coordinates of H_i^1 w.r.t. LFCS_1 denoted as $\mathbf{H}_{1i}^{LF1} = \begin{bmatrix} x_{h1i}^{LF1} & y_{h1i}^{LF1} & z_{h1i}^{LF1} \end{bmatrix}^{\mathrm{T}}$, $i = 1,2,3$, can be calculated with equations (4), (8), and (9).

$$\begin{bmatrix} \left(\mathbf{H}_{1i}^{nLF1}\right)^{\mathrm{T}} & 1 \end{bmatrix}^{\mathrm{T}} = \left(\mathbf{T}_{nLF1}^{S2}\right)^{-1} \begin{bmatrix} \left(\mathbf{H}_{1i}^{S2}\right)^{\mathrm{T}} & 1 \end{bmatrix}^{\mathrm{T}}, \quad i = 1, 2, 3, \tag{8}$$

$$\begin{bmatrix} \left(\mathbf{H}_{1i}^{LF1}\right)^{\mathrm{T}} & 1 \end{bmatrix}^{\mathrm{T}} = \mathbf{T}_{nLF1}^{LF1} \begin{bmatrix} \left(\mathbf{H}_{1i}^{nLF1}\right)^{\mathrm{T}} & 1 \end{bmatrix}^{\mathrm{T}}, \quad i = 1, 2, 3, \tag{9}$$

where $\mathbf{H}_{1i}^{nLF1} = \begin{bmatrix} x_{h1i}^{nLF1} & y_{h1i}^{nLF1} & z_{h1i}^{nLF1} \end{bmatrix}^{\mathrm{T}}$ are the coordinates of H_i^1 w.r.t. ${}^{\mathrm{n}}\mathrm{LFCS}_1$, and $\mathbf{H}_{11}^{LF1} = \mathbf{0}$, $y_{h12}^{LF1} = 0$, $z_{h12}^{LF1} = 0$, and $y_{h13}^{LF1} = 0$.

When PCS_2 is coincident with LFCS_1, $\mathbf{H}_{2i}^{LF1} = \mathbf{H}_{2i}^{P2}$ and the variations of H_i^2, $i = 1,2,3$, w.r.t. SCS_2, are as follows:

$$\begin{aligned} \begin{bmatrix} \left(\mathbf{V}_{h2i}^{S2}\right)^{\mathrm{T}} & 1 \end{bmatrix}^{\mathrm{T}} = {} & \mathbf{T}_{nLF1}^{S2} \left(\mathbf{T}_{nLF1}^{LF1}\right)^{-1} \begin{bmatrix} \left(\mathbf{H}_{2i}^{LF1}\right)^{\mathrm{T}} & 1 \end{bmatrix}^{\mathrm{T}} \\ & - \begin{bmatrix} \left({}^{0}\mathbf{H}_{2i}^{S2}\right)^{\mathrm{T}} & 1 \end{bmatrix}^{\mathrm{T}}, \quad i = 1, 2, 3, \end{aligned} \tag{10}$$

where the coordinates decorated with a superscript "0" represent the nominal ones. Certainly, the variations of H_i^1, $i = 1,2,3$, w.r.t. SCS_2, are $\mathbf{V}_{h1i}^{S2} = \mathbf{H}_{1i}^{S2} - {}^{0}\mathbf{H}_{1i}^{S2}$ and ${}^{0}\mathbf{H}_{1i}^{S2} = {}^{0}\mathbf{H}_{2i}^{S2}$, $i = 1,2,3$.

3.2. Variation Propagation Analysis Incorporating Deformation. When the deformation by the clamping forces of temporary fasteners is incorporated into part-to-part locating process, the variation analysis is a rigid-compliant one. In the part-to-part locating process, the DA holes of Part 2 are fastened with their located DA holes on Part 1, in sequence. Here, compared with the rigid locating process in Section 3.1, it is regarded that when the secondary and tertiary datum holes of Part 2 are fastened with their located DA holes, these DA hole-hole pairs are forced to be coincident with each other. This rigid-compliant locating process is assumed as follows:

(a) PCS_2 is translated and rotated to be coincident with $LFCS_1$

(b) The DOFs of H_1^2 and H_1^1 are tied

(c) H_2^2 and H_2^1 are clamped to be coincident, and then their DOFs are tied

(d) Similarly with (c), H_3^2 and H_3^1 are clamped to be coincident, and then their DOFs are tied

Subprocesses (a) and (b) belong to rigid locating process, while Subprocesses (c) and (d) are compliant one. In Subprocesses (c) and (d), it is assumed that: the clamping forces of the temporary fasteners eliminate the positional differences between the DA hole-hole pairs; the clamping forces are a pair of equal and opposite concentrated forces upon the DA hole-hole pair centers, respectively, as shown in Figure 3.

By referring to equations (5) and (6), the linear relationships between the displacements and forces w.r.t. SCS_2 due to the clamping forces are as follows:

$$\begin{cases} \left[\mathbf{F}_{cF(l\_hi)}^{S2\,\mathrm{T}} \quad \mathbf{F}_{cV(l\_hi)}^{S2\,\mathrm{T}} \right]^{\mathrm{T}} = \mathbf{K}_{(l\_hi)}^{S2} \left[\mathbf{V}_{cF(l\_hi)}^{S2\,\mathrm{T}} \quad \mathbf{V}_{cV(l\_hi)}^{S2\,\mathrm{T}} \right]^{\mathrm{T}}, \\ \mathbf{F}_{cF(l\_hi)}^{S2} = \mathbf{0}, \\ \mathbf{V}_{cV(l\_hi)}^{S2} = \left[\mathbf{V}_{cV(l\_hi)\_f}^{S2\,\mathrm{T}} \quad \mathbf{V}_{cV(l\_hi)\_h}^{S2\,\mathrm{T}} \right]^{\mathrm{T}}, \\ \mathbf{F}_{B(l\_hi)}^{S2} = \mathbf{C}_{(l\_hi)}^{S2} \left[\mathbf{F}_{cF(l\_hi)}^{S2\,\mathrm{T}} \quad \mathbf{F}_{cV(l\_hi)}^{S2\,\mathrm{T}} \right]^{\mathrm{T}}, \quad i = 2, 3, \end{cases} \tag{11}$$

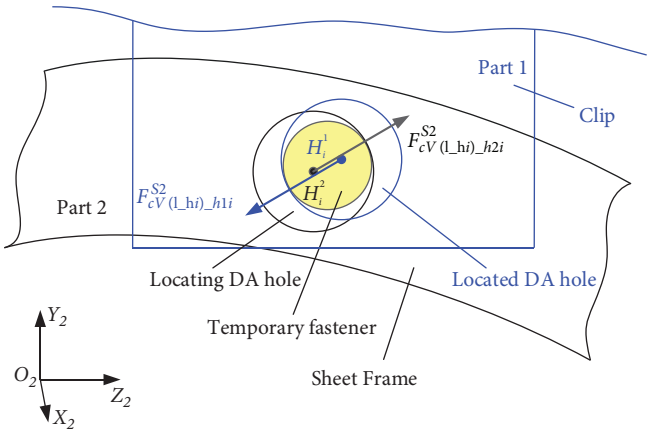

Figure 3: Clamping a DA hole-hole pair by temporary fastener ($i = 2, 3$).

where the subscript "(l_hi)," $i = 2, 3$, represents Subprocess (c) or (d). For Subprocess (c), $i = 2$, the boundary condition is that Part 1 is located by earholes and the DOFs of H_1^2 and H_1^1 are tied. $\mathbf{F}_{cF(l\_h2)}^{S2}$ corresponds to the points free of loads, including the measuring points, the riveting hole centers, the DA hole centers except H_2^1 and H_2^2, etc. The subscript "$\_f$" represents the points located by fixture, except the ones for the boundary condition, and thus, $\mathbf{V}_{cV(l\_h2)\_f}^{S2} = \mathbf{0}$. $\mathbf{V}_{cV(l\_h2)\_h}^{S2} = \left[\mathbf{V}_{cV(l\_h2)\_h12}^{S2\,\mathrm{T}} \quad \mathbf{V}_{cV(l\_h2)\_h22}^{S2\,\mathrm{T}} \right]^{\mathrm{T}}$ denotes the displacements of H_2^1 and H_2^2 by the clamping forces, and then

$$\begin{cases} \mathbf{V}_{cV(l\_h2)\_h12}^{S2} - \mathbf{V}_{cV(l\_h2)\_h22}^{S2} = -\left(\mathbf{V}_{h12}^{S2} - \mathbf{V}_{h22}^{S2} \right), \\ \mathbf{F}_{cV(l\_h2)\_h12}^{S2} = -\mathbf{F}_{cV(l\_h2)\_h22}^{S2}. \end{cases} \tag{12}$$

Thus, $\mathbf{V}_{cV(l\_h2)\_h}^{S2}$, $\mathbf{F}_{cV(l\_h2)}^{S2}$, $\mathbf{V}_{cF(l\_h2)}^{S2}$ and $\mathbf{F}_{B(l\_h2)}^{S2}$ can be calculated with equations (11) and (12).

Similarly, the unknown displacements and forces in Subprocess (d) can be calculated with equations (11) and (13).

$$\begin{cases} \mathbf{V}_{cV(l\_h3)\_h13}^{S2} - \mathbf{V}_{cV(l\_h3)\_h23}^{S2} = -\left(\mathbf{V}_{h13}^{S2} + \mathbf{V}_{cF(l\_h2)\_h13}^{S2} - \mathbf{V}_{h23}^{S2} - \mathbf{V}_{cF(l\_h2)\_h23}^{S2} \right), \\ \mathbf{F}_{cV(l\_h3)\_h13}^{S2} = -\mathbf{F}_{cV(l\_h3)\_h23}^{S2}, \end{cases} \tag{13}$$

where $\mathbf{V}_{cF(l\_h2)\_h13}^{S2}$ and $\mathbf{V}_{cF(l\_h2)\_h23}^{S2}$ denote the displacements of H_3^1 and H_3^2 produced in Subprocess (c). Besides, the boundary condition for Subprocess (d) is that the DOFs of H_2^2 and H_2^1 are tied, based on the boundary condition for Subprocess (c).

4. Variation Analysis of Aircraft Panel Assembly

4.1. Variation Propagation Analysis for the Entire Assembly Process of an Aircraft Panel. The variation propagation

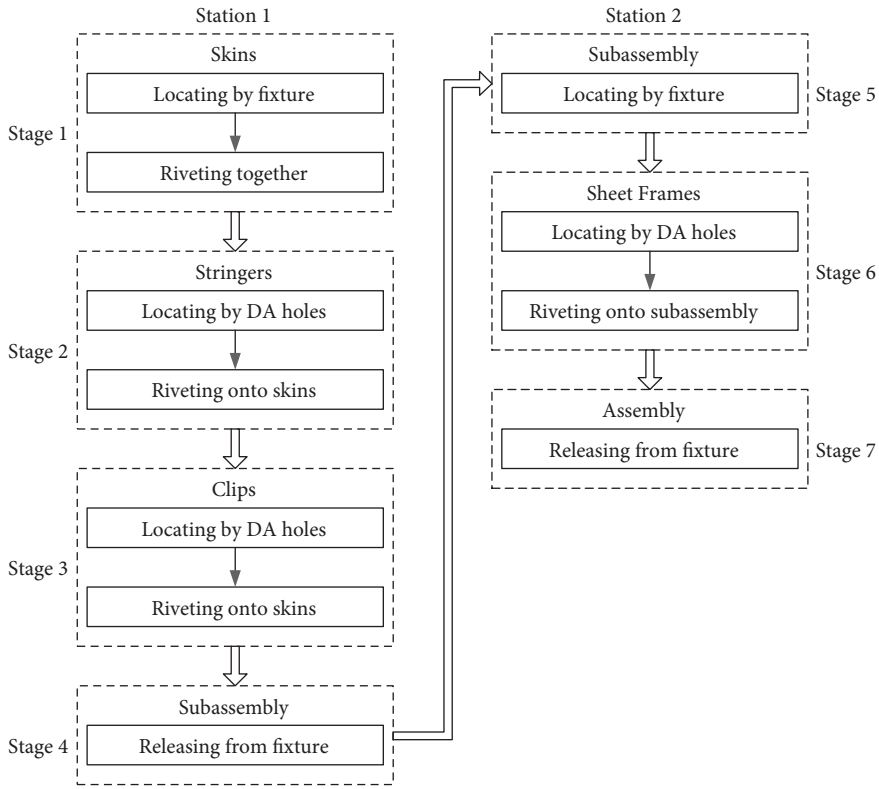

Figure 4: The entire assembly process of an aircraft panel.

analysis for an entire assembly process is performed to describe the relationships between the variations of assembled products and sources. As shown in Figure 4, the entire assembly process of an aircraft panel (seen in Figure 1) can be decomposed into two stations and seven stages, as well as several segmental processes including locating by fixture, locating by DA holes, riveting two parts and releasing from fixture. These processes can be further decompensated into four elementary steps: locate, clamp, join and release [39]. The process of locating by DA holes is studied in Section 3, and the variation propagation for the other three ones is formulated as follows.

4.1.1. Locating by Fixture. The two skins and the subassembly are located by fixture at the beginning of Stations 1 and 2, respectively. The fixtures in the two stations are similar, which both consist of located earholes and fixture boards. Accordingly, the process of locating by fixture contains two subprocesses as follows:

(a) Locating by earholes: the earholes of parts/subassemblies are predrilled, similarly with the DA holes. In Station 1, each of the skins is located by two earholes, which belong to hole-hole joints. This subprocess is assumed to be a rigid locating process, similarly with locating by DA holes not incorporating deformation (seen in Section 3.1). In Station 2, the subassembly is located by four earholes, including two ones for rigid locating and the other two

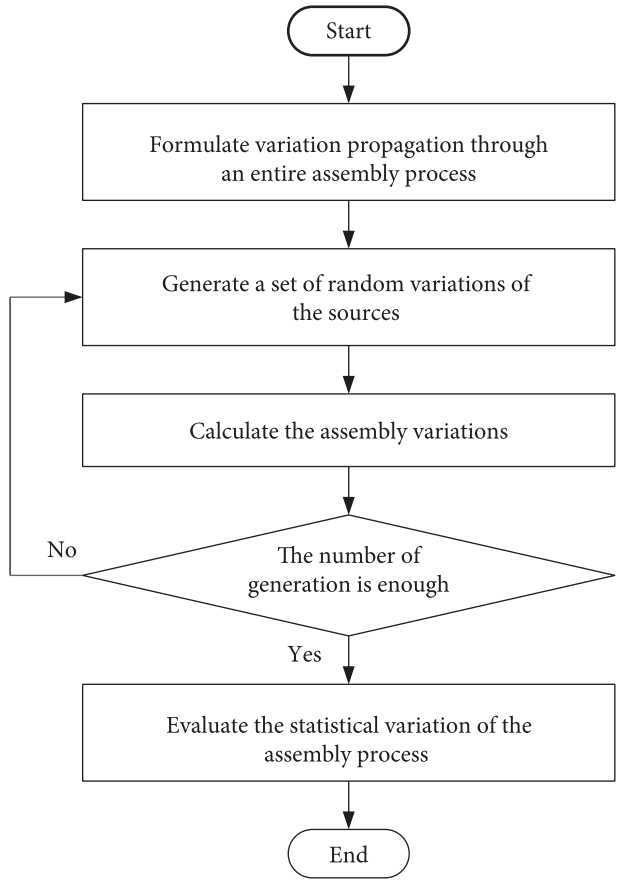

Figure 5: Flow chart of statistical variation analysis.

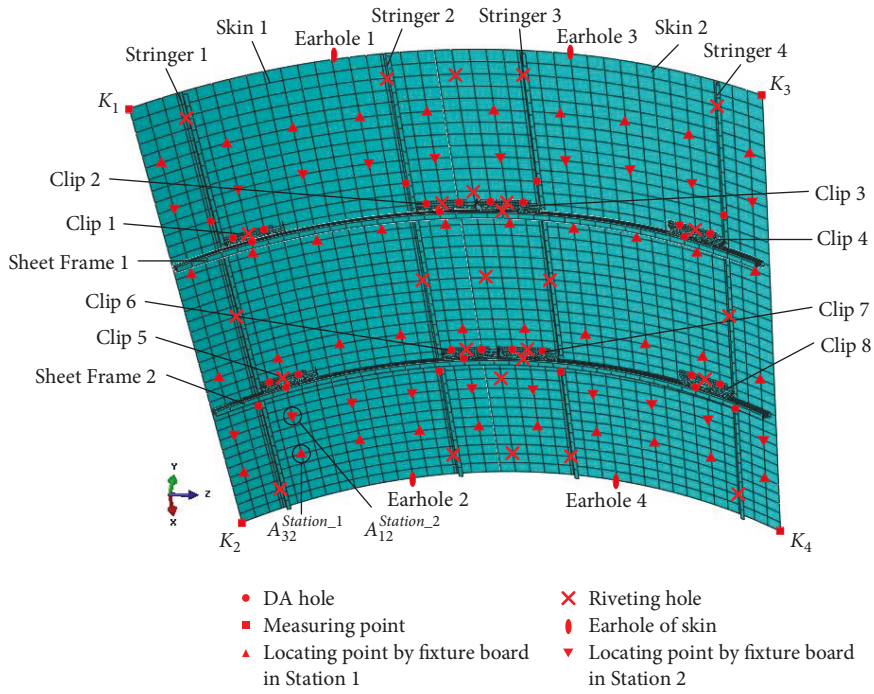

Figure 6: FE model of an aircraft panel.

Table 1: Tolerance schemes of parts and fixture.

Variation sources	Tolerance (mm)				
	Fixture	Skin	Stringer	Clip	Sheet frame
Nonprimary datum locating DA hole/earhole (⌖)		$\phi 0.2$	$\phi 0.2$	$\phi 0.2$	$\phi 0.2$
Located DA hole/earhole (⌖)	$\phi 0.07$	$\phi 0.4$		$\phi 0.4$	
Surface for locating (⌓)		0.4	0.4	0.4	0.4
Surface for located (⌓)	0.13	0.5		0.5	
Surface for riveting (⌓)		0.5	0.4	0.4	0.4
Surface for riveted (⌓)		0.5		0.5	
Surface for measuring (⌓)		0.5			

ones for over constraining the principal surface of skins. The latter is regarded as a compliant locating process, similarly with the process of locating by fixture boards and straps (seen in the next subprocess). Subsequently, all DOFs of the earhole centers are tied to fixture.

(b) Locating by fixture boards and straps: fixture boards and straps are used for over constraining the principal surface of skins. Each fixture board has several small working surfaces. The corresponding locating surfaces on skins are clamped to the working surfaces and constrained by straps. Here, each of the locating surfaces is abstracted as a locating point. This subprocess is a compliant locating process, where the displacements of the locating points w.r.t SCS, denoted as $\mathbf{V}^S_{cV(l\_f)\_f}$, are along the normal directions of principal surface of skins, and then

$$\begin{cases} \left[\mathbf{F}^S_{cF(l\_f)}{}^{\mathrm{T}} \quad \mathbf{F}^S_{cV(l\_f)}{}^{\mathrm{T}}\right]^{\mathrm{T}} = \mathbf{K}^S_{(l\_f)}\left[\mathbf{V}^S_{cF(l\_f)}{}^{\mathrm{T}} \quad \mathbf{V}^S_{cV(l\_f)}{}^{\mathrm{T}}\right]^{\mathrm{T}}, \\ \mathbf{F}^S_{cF(l\_f)} = \mathbf{0}, \\ \mathbf{V}^S_{cV(l\_f)} = \mathbf{V}^S_{cV(l\_f)\_f}, \\ \mathbf{F}^S_{B(l\_f)} = \mathbf{C}^S_{(l\_f)}\left[\mathbf{F}^S_{cF(l\_f)}{}^{\mathrm{T}} \quad \mathbf{F}^S_{cV(l\_f)}{}^{\mathrm{T}}\right]^{\mathrm{T}}, \end{cases} \tag{14}$$

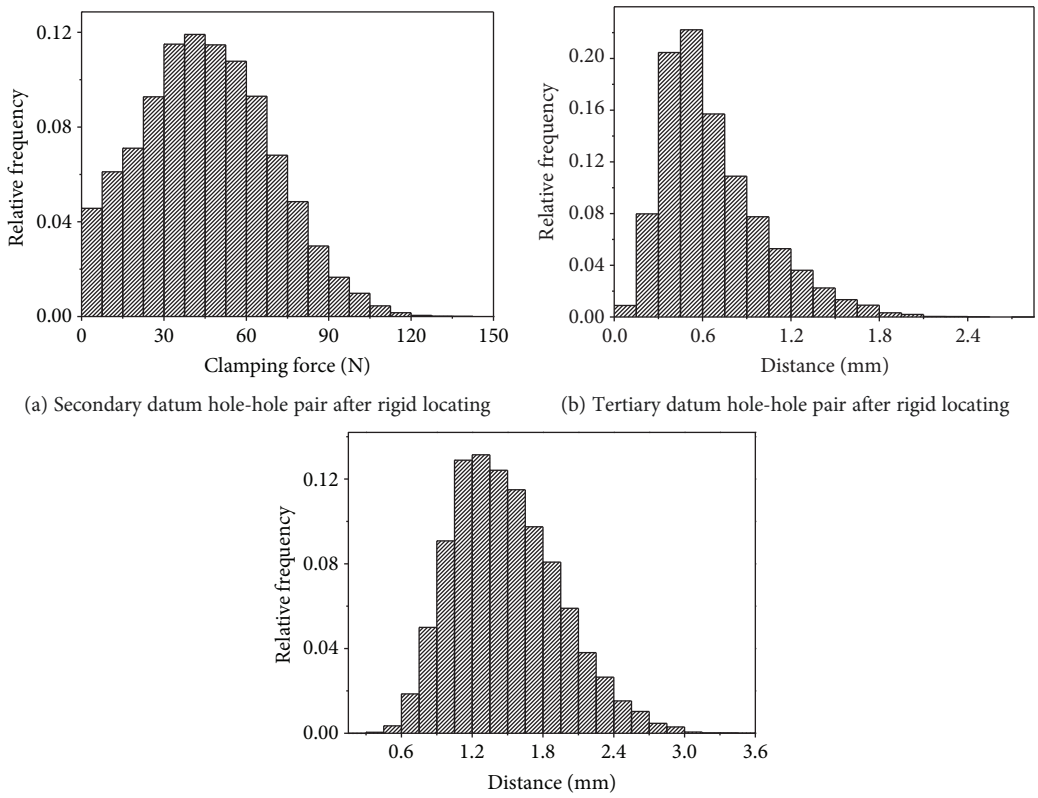

(a) Secondary datum hole-hole pair after rigid locating

(b) Tertiary datum hole-hole pair after rigid locating

(c) Tertiary datum hole-hole pair after fastening secondary datum hole-hole pair

Figure 7: Distributions of distances between nonprincipal datum hole-hole pair centers.

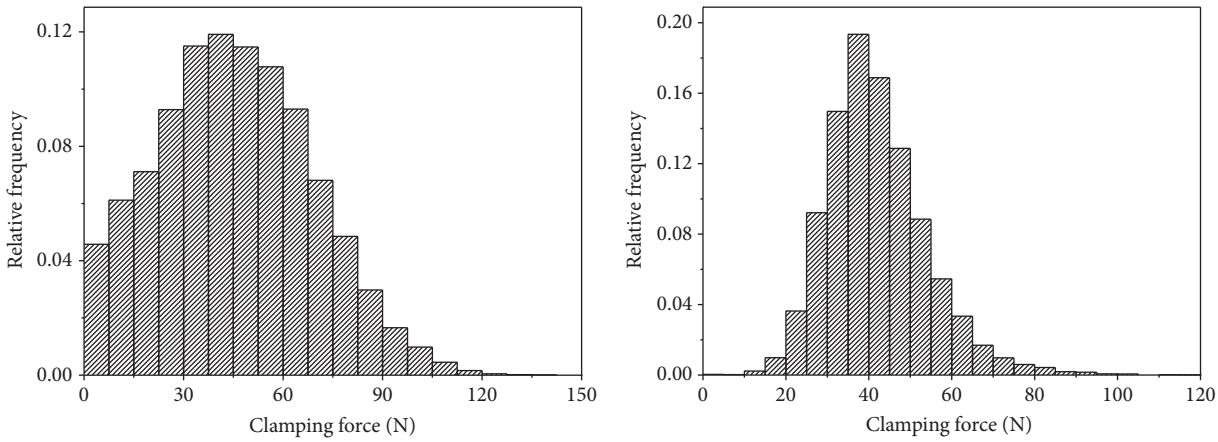

(a) Secondary datum hole

(b) Tertiary datum hole

Figure 8: Distributions of magnitude of clamping forces at nonprincipal datum hole centers.

where the subscript "(l_f)" represents this subprocess. The boundary condition is that the skins or the subassembly is located by earholes.

Then, it is assumed that the out-of-surface translational DOFs of the locating points are constrained by fixture boards and straps.

4.1.2. Riveting Two Parts. In aircraft panel assembly, hammer riveting is often used for joining two parts together. This riveting process contains three steps: clamp, join and release. In particular, the riveting holes have been reamed out to guarantee the concentricity before riveting. For the sake of simplification, it is assumed that all riveting hole-hole pairs in a riveting process are riveted together simultaneously.

Firstly, in the clamp step, the riveting hole centers of the two parts are clamped to certain positions by jacking block and rivet driver. In the riveting process of two skins, the riveting hole centers are clamped to their nominal positions. In the riveting process of a frame part with

Table 2: Statistical characteristics of assembly variations.

Point	Direction	Mean (mm)		Standard deviation (mm)	
		EX1	EX2	EX1	EX2
K_1	x_M	−0.0018	−0.0016	0.0130	0.0156
	y_M	−0.3205	1.0933	0.7163	0.8142
	z_M	0.1410	−0.5727	0.3153	0.3736
	Normal	−0.3458	1.2291	0.7726	0.8847
K_2	x_M	−0.0015	−0.0047	0.0130	0.0156
	y_M	−0.3326	1.1291	0.8639	0.6683
	z_M	0.1297	−0.6150	0.3661	0.3121
	Normal	−0.3499	1.2822	0.9236	0.7295
K_3	x_M	0.0113	0.0453	0.0602	0.1749
	y_M	−0.1437	2.0207	0.8748	0.8938
	z_M	−0.1075	0.8228	0.4400	0.4083
	Normal	−0.1790	2.1441	0.9735	0.9713
K_4	x_M	0.0117	0.0453	0.0603	0.1747
	y_M	−0.2667	2.3695	0.9491	1.2200
	z_M	−0.2062	0.8649	0.5080	0.2727
	Normal	−0.3359	2.4600	1.0656	1.1123

the pre-fixed part/subassembly, the riveting hole centers of the latter are clamped motionless, while the riveting hole centers of the former are clamped to the ones of the latter. Then,

$$\begin{cases} \left[\mathbf{F}^S_{cF(r\_c)}{}^{\mathrm{T}} \quad \mathbf{F}^S_{cV(r\_c)}{}^{\mathrm{T}} \right]^{\mathrm{T}} = \mathbf{K}^S_{(r\_c)} \left[\mathbf{V}^S_{cF(r\_c)}{}^{\mathrm{T}} \quad \mathbf{V}^S_{cV(r\_c)}{}^{\mathrm{T}} \right]^{\mathrm{T}}, \\ \mathbf{F}^S_{cF(r\_c)} = \mathbf{0}, \\ \mathbf{V}^S_{cV(r\_c)} = \left[\mathbf{V}^S_{cV(r\_c)\_f}{}^{\mathrm{T}} \quad \mathbf{V}^S_{cV(r\_c)\_r}{}^{\mathrm{T}} \right]^{\mathrm{T}}, \\ \mathbf{F}^S_{B(r\_c)} = \mathbf{C}^S_{(r\_c)} \left[\mathbf{F}^S_{cF(r\_c)}{}^{\mathrm{T}} \quad \mathbf{F}^S_{cV(r\_c)}{}^{\mathrm{T}} \right]^{\mathrm{T}}, \end{cases} \tag{15}$$

where the subscript "(r_c)" represents the clamp step in the riveting process. The boundary condition is the same with equation (14) for riveting two skins. And in the riveting process of a frame part, the boundary condition is coupled with tying the DOFs of the DA/riveting hole-hole pair centers which are joined before this step. $\mathbf{V}^S_{cV(r\_c)\_f} = \mathbf{0}$. $\mathbf{V}^S_{cV(r\_c)\_r} = \left[\mathbf{V}^S_{cV(r\_c)\_r1}{}^{\mathrm{T}} \quad \mathbf{V}^S_{cV(r\_c)\_r2}{}^{\mathrm{T}} \right]^{\mathrm{T}}$ denotes the displacements of the riveting hole centers on the two parts.

Then, in the join step, the DOFs of the riveting hole-hole pair centers are tied.

Finally, in the release step, jacking block and rivet driver are released. The springback forces at the riveting hole centers are assumed as the counterforces in the clamp step as follows:

$$\begin{cases} \left[\mathbf{F}^S_{cF(r\_r)}{}^{\mathrm{T}} \quad \mathbf{F}^S_{cV(r\_r)}{}^{\mathrm{T}} \right]^{\mathrm{T}} = \mathbf{K}^S_{(r\_r)} \left[\mathbf{V}^S_{cF(r\_r)}{}^{\mathrm{T}} \quad \mathbf{V}^S_{cV(r\_r)}{}^{\mathrm{T}} \right]^{\mathrm{T}}, \\ \mathbf{F}^S_{cF(r\_r)} = -\left(\mathbf{F}^S_{cV(r\_c)\_r1} + \mathbf{F}^S_{cV(r\_c)\_r2} \right), \\ \mathbf{V}^S_{cV(r\_r)} = \mathbf{V}^S_{cV(r\_r)\_f}, \\ \mathbf{F}^S_{B(r\_r)} = \mathbf{C}^S_{(r\_r)} \left[\mathbf{F}^S_{cF(r\_r)}{}^{\mathrm{T}} \quad \mathbf{F}^S_{cV(r\_r)}{}^{\mathrm{T}} \right]^{\mathrm{T}}, \end{cases} \tag{16}$$

where the subscript "(r_r)" represents the release step in the riveting process. The boundary condition is that the DOFs of the riveting hole-hole pair centers are tied, based on the boundary condition for the clamp step. $\mathbf{F}^S_{cF(r\_r)}$ denotes the springback forces $\mathbf{V}^S_{cV(r\_r)\_f} = \mathbf{0}$.

4.1.3. Releasing from Fixture. After the assembly process in a station, the subassembly/assembly is released from fixture. This process contains a release step. Obviously, a subassembly/assembly with a set of full constraints is regarded to be in the absence of external forces. Therefore, releasing from fixture is equated with that the constraints by fixture are released except a set of full constraints. Then,

$$\begin{cases} \mathbf{F}^S_{cF(r)} = \mathbf{K}^S_{(r)} \mathbf{V}^S_{cF(r)}, \\ \mathbf{F}^S_{cF(r)} = \left[\mathbf{F}^S_{cF(r)\_fr}{}^{\mathrm{T}} \quad \mathbf{F}^S_{cF(r)\_nonf}{}^{\mathrm{T}} \right]^{\mathrm{T}}, \end{cases} \tag{17}$$

where the subscript "(r)" represents this releasing process. $\mathbf{F}^S_{cF(r)\_fr}$ denotes the springback forces at the points to be released from fixture, which equal to the accumulated forces before the current step. $\mathbf{F}^S_{cF(r)\_nonf} = \mathbf{0}$ corresponds to the points not located by fixture.

With the remained full constraints by fixture in Station 1 or 2, the coordinates of the measuring points w.r.t SCS are $\mathbf{M}^S_{\mathrm{sub/ass}}$, whose coordinates and variations w.r.t MCS are as follows:

$$\begin{cases} \left[\mathbf{M}^M_{\mathrm{sub/ass}}{}^{\mathrm{T}} \quad 1 \right]^{\mathrm{T}} = \left(\mathbf{T}^S_M \right)^{-1} \left[\mathbf{M}^S_{\mathrm{sub/ass}}{}^{\mathrm{T}} \quad 1 \right]^{\mathrm{T}}, \\ \mathbf{V}^M_{m\_\mathrm{sub/ass}} = \mathbf{M}^M_{\mathrm{sub/ass}} - {}^0\mathbf{M}^{nM}, \end{cases} \tag{18}$$

where $\mathbf{T}^S_M = \mathbf{T}^S_{nM} \left(\mathbf{T}^M_{nM} \right)^{-1}$ is the HTM of MCS w.r.t. SCS. $\mathbf{T}^M_{nM}$ can be obtained according to the method to calculate $\mathbf{T}^{LF1}_{nLF1}$ (seen in Section 3.1).

Eventually, the variation propagation though the entire assembly process of an aircraft panel is formulated by combining the variation propagation models of segmental processes sequentially. The input of the variation propagation analysis for an entire assembly process is the variation sources, while the output is the assembly variations. The variation sources considered in this paper contain the variations

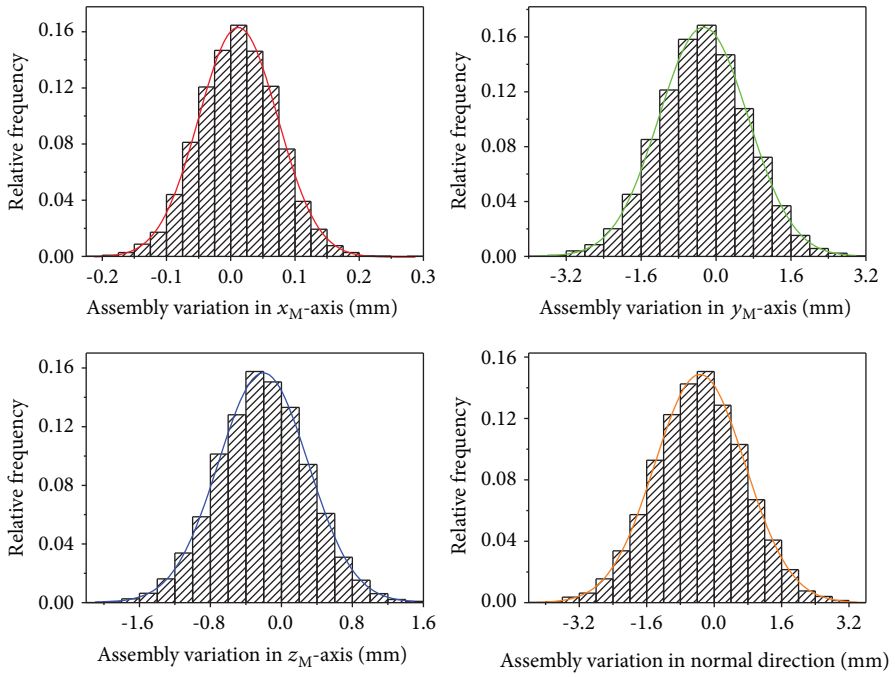

(a) EX1

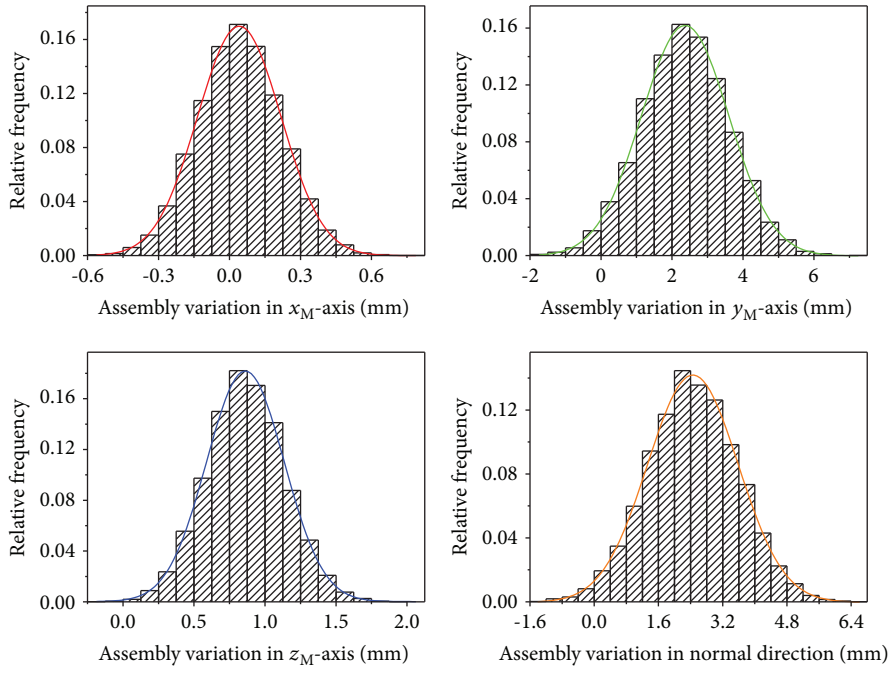

(b) EX2

FIGURE 9: Distributions of assembly variations at K_4.

of parts, fixtures and that caused in riveting process, which denoted by $\mathbf{V}_{\text{part}}^{nP}$, $\mathbf{V}_{\text{fixture}}^{S}$, and $\mathbf{V}_{\text{rivet}}^{S}$, respectively. The relationship between the input and the output can be expressed as follows:

$$\mathbf{V}_{m\_\text{ass}}^{M} = f\left(\mathbf{V}_{\text{part}}^{nP}, \mathbf{V}_{\text{fixture}}^{S}, \mathbf{V}_{\text{rivet}}^{S}\right), \tag{19}$$

where f represents the variation propagation model of the entire assembly process.

4.2. Statistical Variation Analysis with MC Simulation. Because the variations of the sources are generally random variations within their respective tolerance zones, i.e., the assembly process is a random process, statistical analysis is necessary rather than a single case analysis. As one of the

most common methods for statistical analysis, the MC simulation is quite comprehensive and easy to use even for implicit and nonlinear problems, although it is often computationally expensive and time-consuming. This statistical analysis method is used to perform the statistical variation analysis, coupled with the variation propagation model for the entire assembly process of an aircraft panel obtained in Section 4.1. The flow chart of the statistical variation analysis is shown in Figure 5.

Iteratively, a set of random variations of the sources are generated within their tolerance zones and then substituted into the variation propagation model to calculate the assembly variations. The process of random generation and calculation is iterated until the samples are enough. In particular, the generated variations are assumed to be independent of one another and to have a relationship $T = 6\sigma$ with their tolerances under normal distribution.

5. Case Study

5.1. Case Description. The case is the aircraft panel as shown in Figure 1. In order to simplify analysis and save computation time, the number of the frame parts is decreased. As shown in Figure 6, the panel component consists of 2 skins, 4 stringers, 8 clips and 2 sheet frames. Furthermore, it is assumed that (a) SCS_2 is parallel to SCS_1; (b) in Station 2, Earholes 1 and 2 of Skin 1 are used for rigid locating of the subassembly, and thus, the PCS of the subassembly is equated with that of Skin 1; (c) the MCS of subassembly/assembly takes Earholes 1-3 as reference points; (d) the same types of frame parts are assembled simultaneously.

The material of all parts is Al-Li alloy with Young's modulus $E = 73$ GPa, Poisson's ratio $\upsilon = 0.3$. The thickness of parts is 1.8 mm for the skins and clips, 1.2 mm for the stringers, and 1.6 mm for the sheet frames. Each of the skins belongs to single curvature, with the nominal size 2000 mm × 1200 mm and the nominal curvature radius $R =$ 1990 mm.

For the variation sources, the manufacturing tolerances of the parts and fixtures are listed in Table 1. Besides, during the riveting process of Skins 1 and 2, the deviations of clamping positions from their nominal ones are set as ±0.065 mm along the normal direction of the principal skin surface.

ABAQUS is used to construct the FE model with shell element and extract stiffness and coefficient matrices. The computational works in an assembly variation analysis are implemented by MATLAB. The number of iterations in an experiment with MC simulation is set as $N_{MC} = 10000$.

5.2. Validation and Discussion. The proposed method for variation analysis of aircraft panel assembly integrates the deformation by the clamping forces of temporary fasteners into part-to-part locating process. In order to verify the significance of incorporating such deformation, firstly, the positional differences between DA hole-hole pairs and the clamping forces of temporary fasteners are quantified. Then, the analysis results of the experiments without and with the deformation in part-to-part locating process are compared.

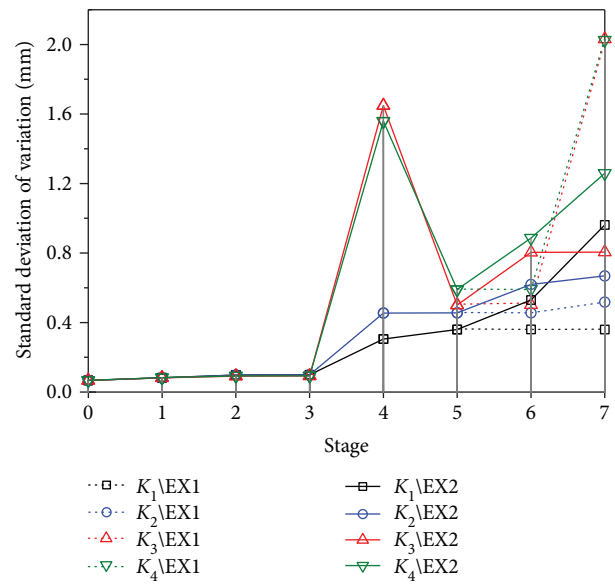

Figure 10: Standard deviations of variations throughout the assembly process.

Two contrast experiments are conducted for the assembly variation analyses incorporating and not incorporating the deformation into the locating process of the sheet frames, which are denoted as EX1 and EX2, respectively. In order to avoid the disturbance of different generated variation sources, the same N_{MC} sets of variation sources are ensured for the two experiments.

In the locating process of sheet frames, by taking Sheet Frame 1 as an example, the distributions of the distances between the centers of nonprincipal datum DA hole-hole pairs are shown in Figure 7, where Figures 7(a) and 7(b) indicate the distance distributions after the rigid locating process of sheet frames, and Figure 7(c) corresponds to the distance between the tertiary datum hole-hole pair centers after the secondary datum hole-hole pairs are fastened in EX2. The distributions of the magnitude of clamping forces at nonprincipal datum hole centers of Sheet Frame 1 in EX2 are shown in Figure 8.

For EX1 and EX2, the statistical characteristics of the assembly variations at K_1~K_4 w.r.t. MCS are compared as shown in Table 2, where the assembly variations along the coordinate axes and the normal direction of the principal skin surface are involved. By taking K_4 as an example, the distributions of the assembly variations are shown in Figure 9. Furthermore, throughout the seven stages of the entire assembly process (by referring to Figure 4), the standard deviations of the variations at K_1~K_4 along the normal direction of the principal skin surface are shown in Figure 10. And the reacting forces/moments by fixture at the earholes and the locating points corresponding to fixture boards are shown in Figure 11, by taking Earhole 2, $A_{32}^{\text{Station\_1}}$ and $A_{12}^{\text{Station\_2}}$ (seen in Figure 6) as examples. In particular, the variations and the forces/moments in Figures 10 and 11 are all measured in SCS_1 or SCS_2, in order to clearly express their changes and trends throughout the entire assembly process.

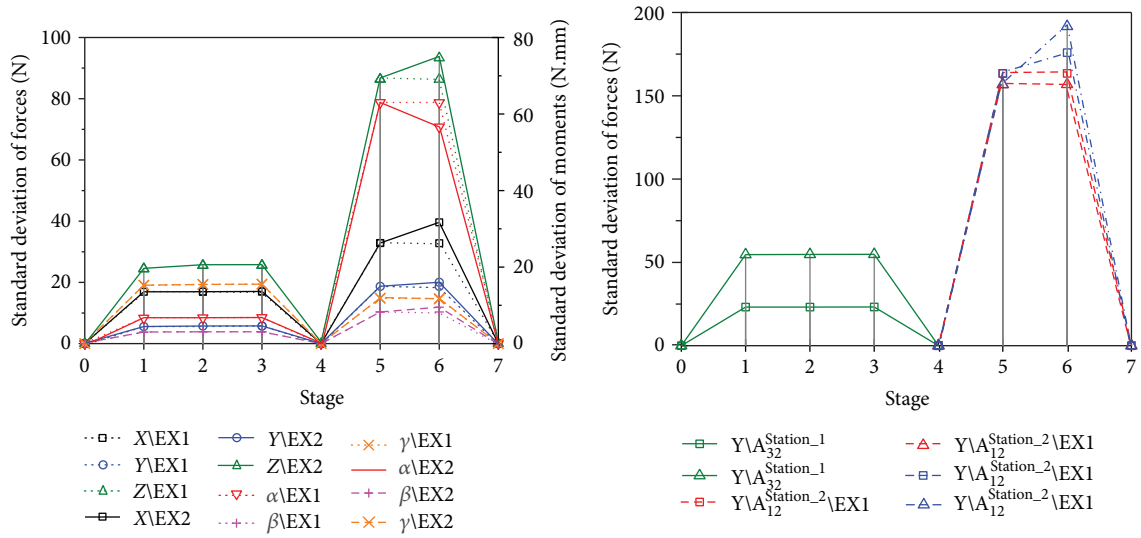

(a) Reacting forces and moments at Earhole 2

(b) Reacting forces at $A_{32}^{\text{Station\_1}}$ and $A_{12}^{\text{Station\_2}}$

Figure 11: Standard deviations of reacting forces/moments by fixture throughout the assembly process.

In addition, for convenience of calculation and measurement, the remained full constraints in Stages 4 and 7 are the constraints at Earhole 1.

From Table 2 and Figures 7–11, it is observed that

(1) The positional differences between the DA hole-hole pair centers of the sheet frames are obvious, and the analysis results of EX1 and EX2 are significantly different. Therefore, the deformation in part-to-part locating process, as well as its influence on the assembly variations, cannot be ignored. Moreover, according to the magnitude of the clamping forces at the DA hole centers, the linear elasticity deformation assumption may be reasonable

(2) In EX2, the positional differences between the tertiary datum hole-hole pair centers are heavily impacted by the process of fastening the secondary datum hole-hole pair. Hence, the locating sequence of DA holes may have a remarkable influence on the deformation of parts/subassemblies in part-to-part locating process and thus the assembly variations

(3) In EX1, the variations at K_1~K_4 are almost unchanged in Stages 1-3 and 5-6, and acutely increased in Stages 4 and 7. This may be because the fixtures in Stations 1 and 2 provide over constraints for the skins and subassembly, respectively, which prevents the deformation of compliant parts/subassemblies by changing the reacting forces/moments by fixture. When the fixtures are released, the reacting forces/moments may cause acute deformation

(4) In Stages 6 and 7 of EX2, the variations at K_1~K_4, as well as the reacting forces/moments by fixture, are changed by comparing with that of EX1. These changes may be due to the clamping forces of temporary fasteners in the locating process of the sheet frames of EX2. The reacting forces/moments by fixture may be increased or reduced in the sheet frame locating process and then further affect the variations as the fixtures are released.

6. Conclusions

This paper presents a rigid-compliant variation analysis method for aircraft panel assembly under part-to-part locating scheme. In part-to-part locating process, the deformation of compliant parts/subassemblies is incorporated, which is caused by the positional differences between DA hole-hole pairs and the clamping forces of temporary fasteners. Based on the kinematic theory and MIC, the variation propagation in part-to-part locating is modeled, according to the practical manufacturing process and reasonable assumption. Furthermore, the entire assembly process of an aircraft panel is divided into several segmental processes, and then, the variation propagations in these segmental processes are formulated and integrated into the variation propagation analysis through the entire assembly process. Finally, the statistical variation analysis is conducted by using MC simulation.

The analysis results of the case study show that (a) for predicting the assembly variations of aircraft panels, the deformation in part-to-part locating process and its influence cannot be ignored; (b) such deformation may be remarkably impacted by the locating sequence of DA holes; (c) the over constraints by fixture prevent large deformation during assembly process of aircraft panels, thus it is necessary to predict the assembly variations out of fixture; and (d) in part-to-part locating process, the clamping forces of temporary fasteners may change the reacting forces/moments by fixture, which may further affect the assembly variations when the assembled panel is released from fixture.

Overall, the proposed method can provide an accurate and reliable prediction for the assembly variations of aircraft panels under part-to-part locating scheme. Besides, it has the potential applications for guiding the assembly operation in part-to-part locating process.

Data Availability

The data used to support the findings of this study are available from the corresponding author upon request.

Conflicts of Interest

The authors declare that there are no conflicts of interest regarding the publication of this paper.

Acknowledgments

The work described in this paper is supported by the National Natural Science Foundation of China under grant nos. (51275236, 51075206, and 51575266) and the Jiangsu Key Laboratory of Precision and Micro-Manufacturing Technology (ZAA1400105).

References

[1] S. J. Hu and J. Camelio, "Modeling and control of compliant assembly systems," *CIRP Annals*, vol. 55, no. 1, pp. 19–22, 2006.

[2] W. Huang and Z. Kong, "Simulation and integration of geometric and rigid body kinematics errors for assembly variation analysis," *Journal of Manufacturing Systems*, vol. 27, no. 1, pp. 36–44, 2008.

[3] J. Jin and J. Shi, "State space modeling of sheet metal assembly for dimensional control," *Journal of Manufacturing Science and Engineering*, vol. 121, no. 4, pp. 756–762, 1999.

[4] R. Mantripragada and D. E. Whitney, "Modeling and controlling variation propagation in mechanical assemblies using state transition models," *IEEE Trans Robot Automat*, vol. 15, no. 1, pp. 124–140, 1999.

[5] Y. Ding, D. Ceglarek, and J. Shi, "Design evaluation of multi-station assembly processes by using state space approach," *Journal of Mechanical Design*, vol. 124, no. 3, pp. 408–418, 2002.

[6] X. Li, J. Shang, and H. Zhu, "An assembly sensitivity analysis method based on state space model," *Assembly Automation*, vol. 37, no. 2, pp. 249–259, 2017.

[7] W. Huang, J. Lin, M. Bezdecny, Z. Kong, and D. Ceglarek, "Stream-of-variation modeling—Part I: a generic three-dimensional variation model for rigid-body assembly in single station assembly processes," *Journal of Manufacturing Science and Engineering*, vol. 129, no. 4, pp. 821–831, 2007.

[8] W. Huang, J. Lin, Z. Kong, and D. Ceglarek, "Stream-of-variation (SOVA) modeling II: a generic 3D variation model for rigid body assembly in multistation assembly processes," *Journal of Manufacturing Science and Engineering*, vol. 129, no. 4, pp. 832–842, 2007.

[9] J. Liu, J. Jin, and J. Shi, "State space modeling for 3-D variation propagation in rigid-body multistage assembly processes," *IEEE Transactions on Automation Science and Engineering*, vol. 7, no. 2, pp. 274–290, 2010.

[10] X. Qu, X. Li, Q. Ma, and X. Wang, "Variation propagation modeling for locating datum system design in multi-station assembly processes," *International Journal of Advanced Manufacturing Technology*, vol. 86, no. 5–8, pp. 1357–1366, 2016.

[11] S. C. Liu and S. J. Hu, "Variation simulation for deformable sheet metal assemblies using finite element methods," *Journal of Manufacturing Science and Engineering*, vol. 119, no. 3, pp. 368–374, 1997.

[12] J. Camelio, S. J. Hu, and D. Ceglarek, "Modeling variation propagation of multi-station assembly systems with compliant parts," *Journal of Mechanical Design*, vol. 125, no. 4, pp. 673–681, 2003.

[13] J. Yue, J. A. Camelio, M. Chin, and W. Cai, "Product-oriented sensitivity analysis for multistation compliant assemblies," *Journal of Mechanical Design*, vol. 129, no. 8, pp. 844–851, 2007.

[14] S. Dahlstrom and L. Lindkvist, "Variation simulation of sheet metal assemblies using the method of influence coefficients with contact modeling," *Journal of Manufacturing Science and Engineering*, vol. 129, no. 3, pp. 615–622, 2007.

[15] K. Xie, L. Wells, J. A. Camelio, and B. D. Youn, "Variation propagation analysis on compliant assemblies considering contact interaction," *Journal of Manufacturing Science and Engineering*, vol. 129, no. 5, pp. 934–942, 2007.

[16] B. Lindau, S. Lorin, L. Lindkvist, and R. Söderberg, "Efficient contact modeling in nonrigid variation simulation," *Journal of Computing and Information Science in Engineering*, vol. 16, no. 1, article 011002, 2016.

[17] K. Yu, S. Jin, X. Lai, and Y. Xing, "Modeling and analysis of compliant sheet metal assembly variation," *Assembly Automation*, vol. 28, no. 3, pp. 225–234, 2008.

[18] H. Chen, C. Tan, and Z. Wang, "Statistical variation analysis of compliant assembly coupling geometrical and material error," *Acta Aeronautica Et Astronautica Sinica*, vol. 9, no. 36, pp. 3176–3186, 2015.

[19] K. Wärmefjord, R. Söderberg, B. Lindau, L. Lindkvist, and S. Lorin, "Joining in nonrigid variation simulation," in *Computer-Aided Technologies-Applications in Engineering and Medicine*, vol. 3, pp. 41–68, INTECH, 2016.

[20] K. Wärmefjord, R. Söderberg, and L. Lindkvist, "Simulation of the effect of geometrical variation on assembly and holding forces," *International Journal of Product Development*, vol. 18, no. 1, pp. 88–108, 2013.

[21] R. Söderberg, K. Wärmefjord, L. Lindkvist, and R. Berlin, "The influence of spot weld position variation on geometrical quality," *CIRP Annals*, vol. 61, no. 1, pp. 13–16, 2012.

[22] S. Moos and E. Vezzetti, "Resistance spot welding process simulation for variational analysis on compliant assemblies," *Journal of Manufacturing Systems*, vol. 37, no. 37, pp. 44–71, 2014.

[23] S. Lorin, L. Lindkvist, and R. Söderberg, "Variation simulation of stresses using the method of influence coefficients," *Journal of Computing and Information Science in Engineering*, vol. 14, no. 1, article 011001, 2014.

[24] R. Söderberg, K. Wärmefjord, and L. Lindkvist, "Variation simulation of stress during assembly of composite parts," *CIRP Annals*, vol. 64, no. 1, pp. 17–20, 2015.

[25] J. Ni, W. Tang, and Y. Xing, "Three-dimensional precision analysis with rigid and compliant motions for sheet metal assembly," *International Journal of Advanced Manufacturing Technology*, vol. 73, no. 5-8, pp. 805–819, 2014.

[26] N. Cai and L. Qiao, "Rigid-compliant hybrid variation modeling of sheet metal assembly with 3D generic free surface," *Journal of Manufacturing Systems*, vol. 41, pp. 45–64, 2016.

[27] H. Cheng, R. Wang, Y. Li, and K. Zhang, "Modeling and analyzing of variation propagation in aeronautical thin-walled structures automated riveting," *Assembly Automation*, vol. 32, no. 1, pp. 25–37, 2012.

[28] J. Lin, S. Jin, C. Zheng, Z. Li, and Y. Liu, "Compliant assembly variation analysis of aeronautical panels using unified substructures with consideration of identical parts," *Computer-Aided Design*, vol. 57, pp. 29–40, 2014.

[29] B. Zheng, H. Yu, and X. Lai, "Assembly deformation prediction of riveted panels by using equivalent mechanical model of riveting process," *International Journal of Advanced Manufacturing Technology*, vol. 92, no. 5–8, pp. 1955–1966, 2017.

[30] J. Hartmann, C. Meeker, M. Weller et al., "Determinate assembly of tooling allows concurrent design of Airbus wings and major assembly fixtures," in *SAE Technical Paper Series*, 2004.

[31] L. Irving, S. Ratchev, A. Popov, and M. Rafla, "Implementing determinate assembly for the leading edge sub-assembly of aircraft wing manufacture," *SAE International Journal of Aerospace*, vol. 7, no. 2, pp. 246–254, 2014.

[32] W. Zhang, Z. Wang, C. Tan, and X. Liu, "Assembly variation optimization of aircraft compliant parts based on active locating compensation of fixture," *Acta Aeronautica Et Astronautica Sinica*, vol. 38, no. 6, article 420862, 2017.

[33] H. Li, H. Zhu, P. Li, and F. He, "Tolerance analysis of mechanical assemblies based on small displacement torsor and deviation propagation theories," *International Journal of Advanced Manufacturing Technology*, vol. 72, no. 1–4, pp. 89–99, 2014.

[34] S. Jin, H. Chen, Z. Li, and X. Lai, "A small displacement torsor model for 3D tolerance analysis of conical structures," *Proceedings of the Institution of Mechanical Engineers, Part C: Journal of Mechanical Engineering Science*, vol. 229, no. 14, pp. 2514–2523, 2015.

[35] C. Mickaël and A. Bernard, "3D ISO manufacturing specifications with vectorial representation of tolerance zones," *International Journal of Advanced Manufacturing Technology*, vol. 60, no. 5–8, pp. 577–588, 2012.

[36] H. Li, H. Zhu, X. Zhou, P. Li, and Z. Yu, "A new computer-aided tolerance analysis and optimization framework for assembling processes using DP-SDT theory," *International Journal of Advanced Manufacturing Technology*, vol. 86, no. 5–8, pp. 1299–1310, 2016.

[37] D. E. Whitney, O. L. Gilbert, and M. Jastrzebski, "Representation of geometric variations using matrix transforms for statistical tolerance analysis in assemblies," *Research in Engineering Design*, vol. 6, no. 4, pp. 191–210, 1994.

[38] A. Desrochers and A. Rivière, "A matrix approach to the representation of tolerance zones and clearances," *The International Journal of Advanced Manufacturing Technology*, vol. 13, no. 9, pp. 630–636, 1997.

[39] M. Chang and D. C. Gossard, "Modeling the assembly of compliant, non-ideal parts," *Computer-Aided Design*, vol. 29, no. 10, pp. 701–708, 1997.